pubs.acs.org/Biomac

Article

Bisphosphonate-Conjugated Photo-Crosslinking Polyanionic Hyaluronic Acid Microbeads for Controlled BMP2 Delivery and Enhanced Bone Formation Efficacy

Ratchapol Jenjob, Hong-Phuong Nguyen, Min-Kyoung Kim, Yixin Jiang, Jung Joo Kim, and Su-Geun Yang*

Cite This: *Biomacromolecules* 2021, 22, 4138–4145

Read Online

ACCESS | Metrics & More | Article Recommendations | Supporting Information

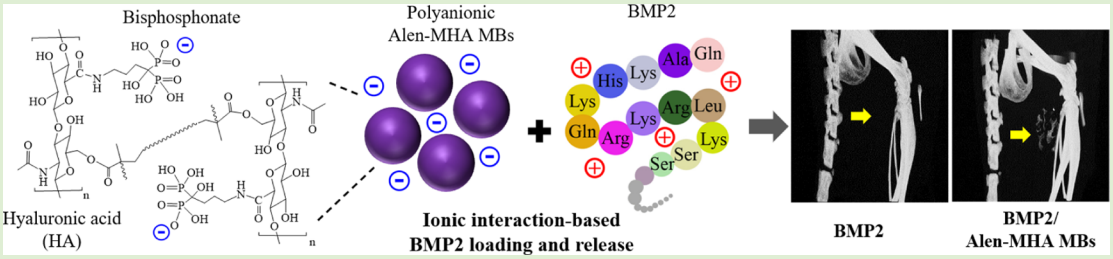

ABSTRACT: In this study, we designed bisphosphonate-conjugated polyanionic hyaluronic acid (HA) microbeads (MBs) for the controlled delivery of bone morphogenetic protein 2 (BMP2). MBs were prepared via the photo-crosslinking of bisphosphonate (alendronate)-conjugated methacrylated HA (Alen-MHA). The polyanionic Alen-MHA MBs actively absorbed cationic BMP2 up to 91.0% of the loading efficacy and displayed a sustained release of BMP2 for 10 days. BMP2/Alen-MHA MBs induced osteogenic-related genes in cellular experiments and showed the highly increased bone formation efficacy in thigh muscle injection and rat spinal fusion animal models. Thus, BMP2/Alen-MHA MBs provide a promising opportunity to improve the delivery efficiency of BMP2.

1. INTRODUCTION

Bone morphogenetic proteins (BMPs) belong to the transforming growth factor-β superfamily and act primarily as bone-inducing autocrine molecules for embryogenesis, bone formation, and remodeling processes in the body.[1] So far, 20 BMP family members have been identified after the first discovery of BMP in 1965.[2] Among them, BMP2 is the only approved drug by the US Food and Drug Administration for the treatment of single-level anterior lumbar interbody fusion (ALIF), tibial nonunion, and oral maxillofacial reconstruction. BMP2 induces osteogenic markers, such as alkaline phosphatase (*ALP*), osteocalcin (*OCN*), and Runt-related transcription factor 2 (*RUNX2*), eventually inducing bone-constructing effects.[3]

The clinical applications of BMP2 have significantly increased over the decades. BMP2 is currently prescribed for more than 50% of all ALIFs and displays substantial therapeutic efficacy. Consequently, the off-label application of BMP2 has been increased. Especially, BMP2 applications in a range of orthopedic procedures have aroused serious safety issues and complications. The reported major complications are ectopic/heterotopic bone formation, uncontrolled bone growth, postoperative nerve root compression, overgrowth of the throat tissue, and compression of the airway.[4−6] Aaron et al. reported that these complications are mainly due to failure in medication control, such as, off-target tissue application, over-dosing, and excessive diffusion of BMP2 into the surrounding tissues.[7] When applied with conventional collagen sponge, BMP2 rapidly diffuses out from the carrier and spreads to nearby tissues. The excessive diffusion of BMP2 leads to a drastic reduction in the local concentration of BMP2, rapid loss of activity at the injection site, and overgrowth of the nontarget surrounding tissues.[1,7,8] Therefore, one of the major challenges of BMP2 therapy is the optimized delivery system that can exactly apply the titrated dose to the bone defects and also can release the BMP2 at the site of implantation without devastating leakage to other tissues.[9]

To date, many materials have been screened to get the optimized delivery system of BMP2, including collagen,[10] chitosan, poly(deoxyribose) isobutyrate,[11] alginate, hydrogel,[12] collagen sponge,[13] and core−shell nanofibers.[14] One of them, hyaluronic acid (HA), exhibits excellent biocompatibility and synergistic effects on bone formation when BMP2 is applied.[9,15]

Bisphosphonates are classified as stable pyrophosphonate analogues. They enhance the bone-binding properties via

Received: May 14, 2021
Revised: July 22, 2021
Published: August 4, 2021

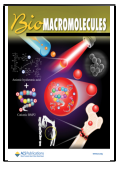

https://doi.org/10.1021/acs.biomac.1c00610
Biomacromolecules 2021, 22, 4138–4145

tridentate binding to calcium and influence bisphosphonates' antiresorptive activity. Bisphosphonates are used for the treatment of diseases associated with the bone and also used in conjunction with anticancer drugs for selected types of cancer treatment.[16] Bisphosphonates are classified into three generations. Alendronate (Alen) is one of the generations that is administered orally for the treatment of bone diseases such as Paget's disease, osteoporosis, malignant hypercalcemia, and metastatic bone disease. However, the most critical disadvantage of Alen is low oral bioavailability.[17] For these reasons, recent research on Alen has been focusing on increasing its bioavailability by formulation of a delivery and release system.

HA is an inherent natural polymer found in all the connective tissues of the body, such as the early fracture callus, cytoplasm of osteoprogenitor cells, and lacunae surrounding hypertrophic chondrocytes in the growth plate. In addition, HA does not exhibit a deleterious immune response often observed in collagen carriers.[9,18] However, in light of recent clinical reports, the functional design of HA polymers for BMP carriers remains a challenging issue.[1,19]

In this study, we prepared HA-based polyelectrolyte microbeads (MBs) as carriers of BMP2. To prepare polyelectrolyte MBs, HA was functionalized with a methacryl moiety (methacrylated HA; MHA) for the UV-curing preparation of MBs and then introduced with anionic bisphosphonate molecules (alendronate; Fosamax, Merck & Co., Inc., NJ). Thus, negatively charged MBs can form ionic complexes with cationic BMP2. The cytotoxicity and tissue compatibility of Alen-MHA MBs were evaluated. Furthermore, we examined BMP2 loading and the release of Alen-MHA MBs using *in vitro* assay methods. The osteogenic effect of Alen-MHA MBs was examined using osteoblast cells in terms of osteogenic gene expression. The bone formation and spinal fusion effects of Alen-MHA MBs were evaluated using *in vivo* animal models.[20]

2. EXPERIMENTAL SECTION

2.1. Materials. HA (160 kDa) was purchased from Bioland (Chungju, Korea). Tetra-*n*-butylammonium hydroxide (TBA, 40% w/w aqueous solution) was purchased from Alfa Aesar (Haverhill, MT). BMP2 (purity: > 95%) was obtained from Cowellmedi Co., Ltd., South Korea. Alendronate sodium was purchased from Daehe Biopharma (Daejeon, Korea). Methacrylic anhydride, Irgacure 2959, toluidine blue O (TBO), Span 20, and cetylpyridinium chloride (CPC) were purchased from Sigma-Aldrich (St. Louis, MO). Medium-chain triacylglyceride (MCT) oil was obtained from Nisshin Oil Mill. Alizarin Red S, 2% w/v solution (pH 4.2), was obtained from Electron Microscopy Sciences, USA.

2.2. Photo-Crosslinking Preparation of Alen-MHA MBs Using Capillary Microfluidics. First, the Alen-MHA polymer for the preparation of Alen-MHA MBs was synthesized following reported methods and then introduced to a capillary microfluidic device[21] (please refer to the Supporting Information). The microfluidic device was made using glass capillary tubes with two channels of the dispersed phase and the continuous phase, as previously reported.[22,23] A syringe pump was used to flow both phases through the channels. The Alen-MHA polymer solution containing 200 mg in 2 mL of 0.4% Irgacure 2959 was introduced into the internal phase at a flow rate of 30 μL/min. MCT oil containing 0.1% Span 20 was used as a continuous phase and injected into the outside channel at a flow rate of 200 μL/min. Droplets of the polymer solution were formed at the end tip of the capillary tube and then crosslinked under UV light (80 W). The obtained beads were washed with 70% ethanol several times and then stored in 70% ethanol overnight for dehydration. The morphology and size of Alen-MHA MBs were characterized using scanning electron microscopy (SEM, model S800, Hitachi, Tokyo, Japan). The beads were dried overnight at room temperature and then placed on an aluminum stub and coated with platinum. Coated samples were observed using a scanning electron microscope at 15 kV.

2.3. Ionic Charge Characterization of Alen-MHA MBs. The surface charge of Alen-MHA MBs was evaluated using TBO dye following a previous report.[24] The beads were stained with 600 μL of 0.1 mM TBO with shaking for 1 h. The bead color was observed using a stereomicroscope (SX61; Olympus Life Science, Tokyo, Japan).

2.4. BMP2 Loading and Release from Alen-MHA MBs. BMP2 loading and release were calculated as previously reported.[22,25] Recombinant human BMP2 was reconstituted at 250 μg/mL in sterile water, and single-use aliquots were frozen until use. For the loading study, 0.5 mL of 25 μg/mL BMP2 was added to 40 MBs. The MBs were then shaken at 37 °C, and the supernatant was collected at predetermined time intervals. The residual concentration of BMP2 in the supernatants was measured using a BMP2 ELISA kit (PeproTech, 900K255EK-02, VA). Additionally, fluorescein isothiocyanate (FITC)-labeled BMP2 was prepared following a previously reported method.[23] The active absorption of FITC-BMP2 by the MBs was observed using a fluorescence microscope (BX 51, Olympus Life Science, Tokyo, Japan).

For the release study, BMP2-loaded MBs were immersed in 1 mL of phosphate-buffered saline (PBS) (pH 7.4) and shaken at 100 rpm at 37 °C, and the supernatant was collected for the estimation of the released amount. The amount of released BMP2 was evaluated using the BMP2 ELISA kit (PeproTech, 900K255EK-02, VA).

2.5. Cellular Toxicity and Tissue Compatibility Studies. The cellular toxicity of the prepared MBs was determined against MC3T3-E1 cells (Korea Cell Line Bank, Seoul, Korea) using the WST-1 assay kit (Abcam plc., Cambridge, UK). MC3T3-E1 cells were plated in 24-well plates with Dulbecco's modified Eagle's medium (Cellgro, Manassas, VA) containing 4.5 g/mL glucose, 10% v/v fetal bovine serum (Atlanta Biologics, Atlanta, GA), 1% v/v 10,000 IU penicillin/10,000 μg/mL streptomycin (Mediatech, Manassas, VA), and 1% v/v 200 mM L-glutamine. Then, MBs were added to the plates and incubated for 24, 48, and 72 h at 37 °C. The cellular toxicity of the MBs was determined by adding WST-1 to each well and incubating for an additional 30 min. Cell viability was measured at 450 nm using a microplate reader (xMark microplate spectrophotometer, Bio-RAD Inc., Hercules, CA, USA). Cytotoxicity of the beads was calculated as the percentage cell viability (measured as WST-1 reduction) compared with that of the controls.

The tissue compatibility of MBs was measured after the implantation of MBs into rat thigh muscle pouches.[26] 2 weeks after bead implantation, muscle specimens were fixed with 10% buffered formalin and embedded in paraffin. The specimen was then sectioned at a thickness of 3 μm, stained using hematoxylin and eosin (H&E) and Masson trichrome (MT), and imaged using a Leica SCN 400 (DM 2500, Wetzlar, Germany).

2.6. *In Vitro* Cellular Osteogenic Marker Induction Study by Release Control. The bone formation effect of BMP2/Alen-MHA MBs was evaluated based on osteogenic marker induction in MC3T3-E1 cells. MC3T3-E1 cells were seeded in 6-well plates at a density of 1×10^5 cells/well. BMP2/Alen-MHA MBs were applied to each well on day 1 after sterilization under UV light. Cells were divided into two groups according to the treatment protocol (i.e., single treatment or multiple treatments). For single treatment, four Alen-MHA MBs containing a total dose of 500 ng of BMP2 (125 ng BMP2 per one MB) were added to each well at day 1 and maintained for 12 days. In the case of multiple treatments, one Alen-MHA MB containing 125 ng of BMP2 was applied four times a day for 3 days. The total BMP2 dose was adjusted to 500 ng for 12 days. The medium was changed every 3 days before the application of MBs. Cells were recovered after 3, 6, and 9 days of incubation for reverse transcriptase quantitative real-time polymerase chain reaction (RT-qPCR). Total RNA was extracted using TRIsure (Bioline, UK) and reverse-transcribed into cDNA using a Tetro cDNA Synthesis Kit (Bioline, UK). cDNA was amplified using real-time PCR with oligonucleotide primer pairs. Osteoblast differentiation was evaluated by RT-qPCR by examining marker genes, including *Runc2*, *Alp*, and *Ocn*.[26]

2.7. *In Vitro* Cellular Mineralization Study. Cellular mineralization studies were performed using MC3T3-E1 cells.[26] The cells were cultured in 6-well plates, treated with BMP2/Alen-MHA MBs, and

https://doi.org/10.1021/acs.biomac.1c00610
Biomacromolecules 2021, 22, 4138−4145

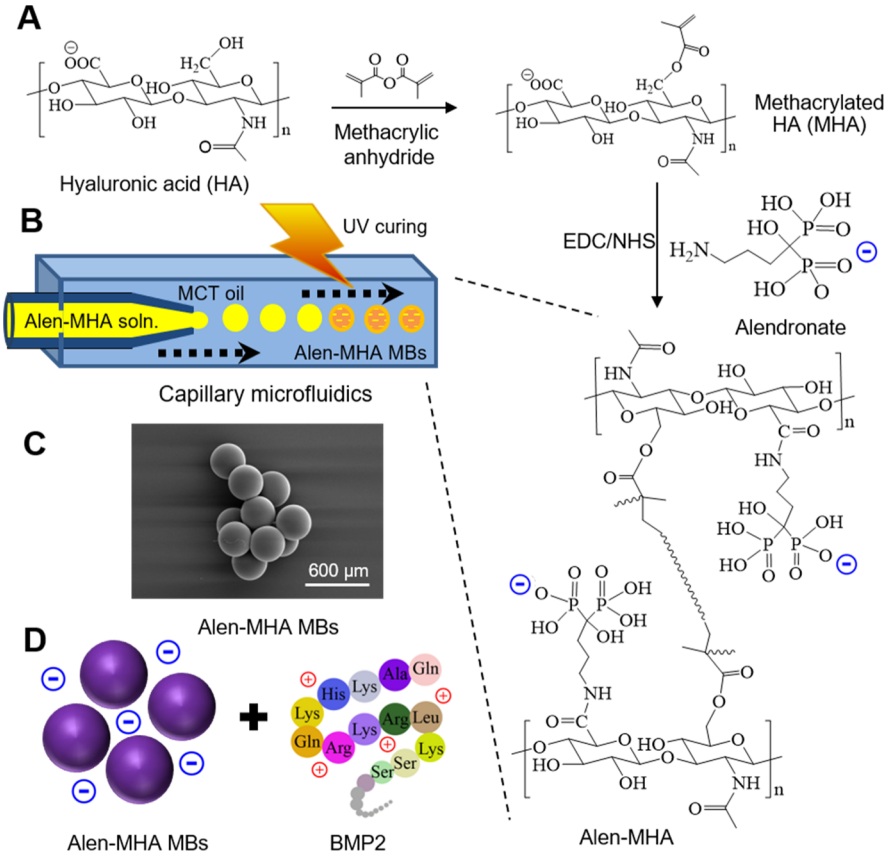

Figure 1. Fabrication of bisphosphonate-mediated anionic polyelectrolyte MBs for ionic interaction-based BMP2 delivery. (A) Schematic illustration of the synthetic process of the Alen-MHA polymer for microfluidic photo-crosslinking fabrication of MBs. (B) UV-photo-crosslinking fabrication of MBs in a flow-focused capillary microfluidic device. (C) SEM image of Alen-MHA MBs. (D) Ionic interaction-based BMP2 loading on Alen-MHA MBs.

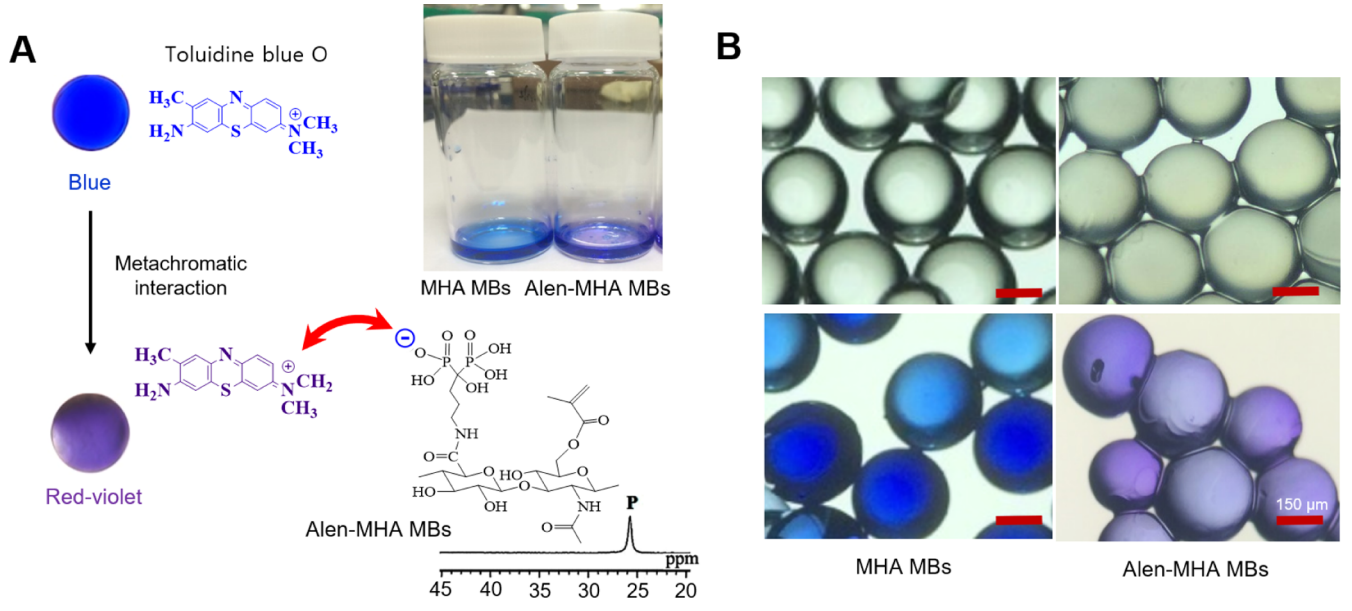

Figure 2. Anionic property of bisphosphonate-mediated polyelectrolyte MBs. (A) TBO tests of MHA and Alen-MHA MBs and ^{31}P NMR spectrum of the synthesized Alen-MHA polymer. (B) Photo-microscopic images of MHA MBs and Alen-MHA MBs. MBs were imaged with or without TBO staining. MHA MBs are blue colored, and anionic Alen-MHA MBs are violet colored.

recovered for Alizarin Red S staining at the last day of incubation. The cells were washed with PBS, fixed with 4% formaldehyde for 30 min, washed twice with distilled water, and stained with Alizarin Red S. For quantitative analysis of the cellular disposition amount of calcium, the cultures were destained with 10% CPC in 10 mM sodium phosphate (final pH 7) for 30 min. The extracted cells were centrifuged at 1500 rpm for 3 min. The supernatant was collected and diluted 10-fold in a 10% CPC solution, and the Alizarin Red S concentration was

https://doi.org/10.1021/acs.biomac.1c00610
Biomacromolecules 2021, 22, 4138−4145

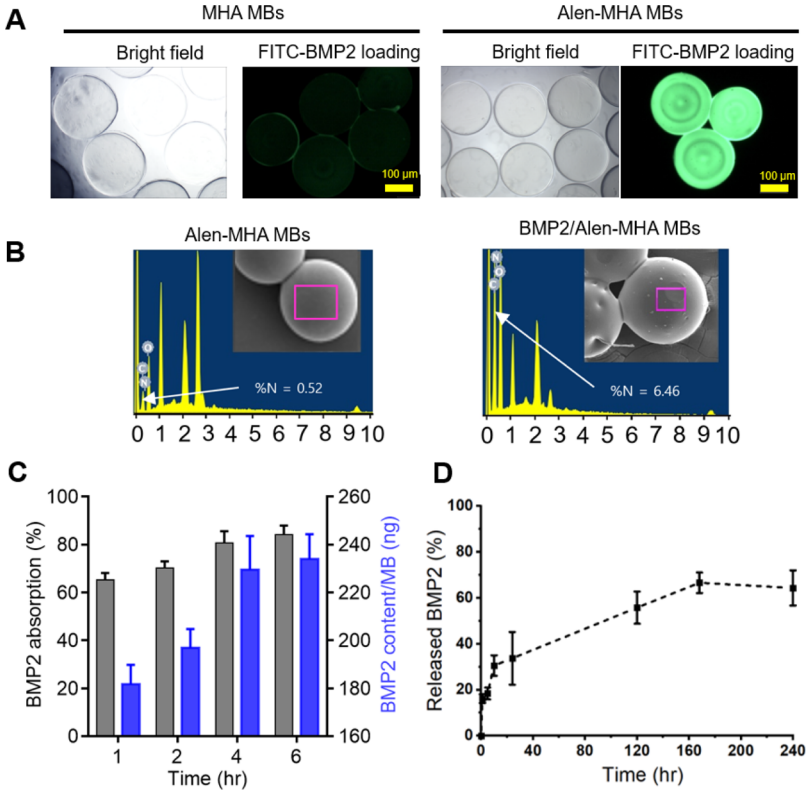

Figure 3. BMP2 loading and release properties of Alen-MHA MBs. (A) Fluorescence phase images after FITC-BMP2 loading on MHA MBs and Alen-MHA MBs. (B) EDX spectra of MHA MBs, Alen-MHA MBs, and BMP2/Alen-MHA MBs. (C) Time-dependent cumulative loading profile of BMP2 on Alen-MHA MBs (n = 5, mean ± sd). (D) Time-dependent BMP2 release profile from Alen-MHA MBs (0−240 h) (n = 3, mean ± sd).

determined by the absorbance measurement at 540 nm on a microplate reader.

2.8. Bone Formation Study in the Mouse Thigh Muscle Pouch. All the animal experiments were performed at the Animal Research Laboratory at Inha University and approved by the Inha University's Animal Care Committee (HI14C0797). All the animal procedures were conducted in accordance with the guidelines issued for animal experimentation at our institute. All the procedures were conducted as previously described.[27,28] For the study, mice (BALB/c, Orient Bio Co., Seongnam, Korea) were divided into four groups: (1) untreated; (2) Alen-MHA MBs; (3) BMP2; and (4) BMP2/Alen-MHA MBs. The treatment of the dose was 20 μg of BMP2. Mice were placed on a surgical table and anesthetized with a continuous inhalation of 2% isoflurane. After a longitudinal incision along with the hind limb, the muscle fibers were separated within the biceps femoris to open a 4 mm deep pocket. The MB samples were applied to the created muscle pouch. Then, the muscle pouch and skin were closed using a 5−0 Vicryl suture. 4 weeks after implantation, bone formation was observed using microcomputed tomography (micro-CT; SkyScan-1072, Belgium). The thigh muscle tissues were recovered and processed for HE and MT staining.

2.9. Statistical Analysis. All data are presented as the mean ± standard error (S.E.M) or mean ± (STDEV). The statistical significance between the groups was determined using Student's t-test and was considered significant when p values were <0.05.

3. RESULTS

3.1. Physicochemical Characteristics of Alen-MHA MBs. Alen-MHA MBs were prepared using a capillary microfluidic device (Figure 1). The successful synthesis of photo-crosslinking polymers (MHA and Alen-MHA) was confirmed using ^{1}H nuclear magnetic resonance (NMR) spectroscopy, Fourier-transform infrared (FTIR) spectroscopy, and inductively coupled plasma-optical emission spectrometry (ICP-OES) (Figures S1-S4). Figure 1C shows that the Alen-MHA MBs have spherical, smooth surfaces, and uniform sizes after photo-crosslinking. The size of Alen-MHA MBs in the dry state, examined under a scanning electron microscope was 319 ± 15 μm. The size distribution of MHA and Alen-MHA MBs is shown in Figure S5.

3.2. Anionic Charge of Alen-MHA MBs. The introduction of bisphosphonates into the MHA polymer was confirmed using the TBO assay. As shown in Figure 2A,B, photo and microscopic observation prove that Alen-MHA Bs changed their color from blue to violet, whereas MHA MBs maintained their blue color. TBO changes from blue to violet after ionic interactions with the anionic Alen-MHA MBs. This metachromasia is attributed to the interaction of cationic TBO at sites of high density of anionic groups.[29−31] ^{31}P NMR spectroscopy strongly supported the presence of phosphates in the Alen-MHA polymer at 25.8 ppm (Figure 2A). The estimated content of phosphorus was 2.40 ± 0.21% (Figure S4).

3.3. BMP2 Loading and Release Property of Alen-MHA MBs. *3.3.1. Ionic Interaction-Based BMP2 Loading on Alen-MHA MBs.* As shown in Figure 3A, fluorescence microscopy revealed that Alen-MHA MBs exhibited a strong green fluorescence after incubation with FITC-labeled BMP2, whereas MHA MBs displayed barely observable green fluorescence. These data suggest that BMP2 loading was based on the ionic interaction mechanism between anionic polyelectrolyte MBs and cationic BMP2. The presence of BMP2 on the Alen-MHA MBs was confirmed by increasing the percentage of nitrogen atoms from 0.62 to 6.46%, as observed in the energy-dispersive X-ray analysis (EDX) results (Figure 2B). The uptake of BMP2 by Alen-MHA MBs was very quick and it increased over time

https://doi.org/10.1021/acs.biomac.1c00610
Biomacromolecules 2021, 22, 4138−4145

(Figure 3C). After 1 h of incubation, approximately 67% of BMP2 was loaded onto the Alen-MHA MBs. The loading efficiency reached 91% after 5 h of incubation. The loading amount of BMP2 per MB reached 250 ng after 5 h of incubation.

3.3.2. Release of BMP2 from Alen-MHA MBs. Figure 3D shows the release profiles of BMP2 from Alen-MHA MBs for up to 10 days. Alen-MHA MBs showed approximately 33% of the initial burst release over 24 h of incubation. After the initial burst release, BMP2 was released in a sustained manner at approximately 3.3% of the total loading amount per day for 10 days. By the end of the release study, nearly 60% of BMP2 was released from the Alen-MHA MBs.

3.4. Cytotoxicity and Tissue Compatibility of Alen-MHA MBs. The cytotoxicity of MBs against MC3T3-E1 cells was also evaluated. As shown in Figure 4A,C, Alen-MHA MBs did not show cytotoxicity after 24, 48, and 72 h of incubation. In particular, most cells incubated with Alen-MHA MBs displayed a green fluorescence in live and dead cell staining, suggesting that the exposed cells remained alive (green) without any apoptotic death (red) (Figure 4C).

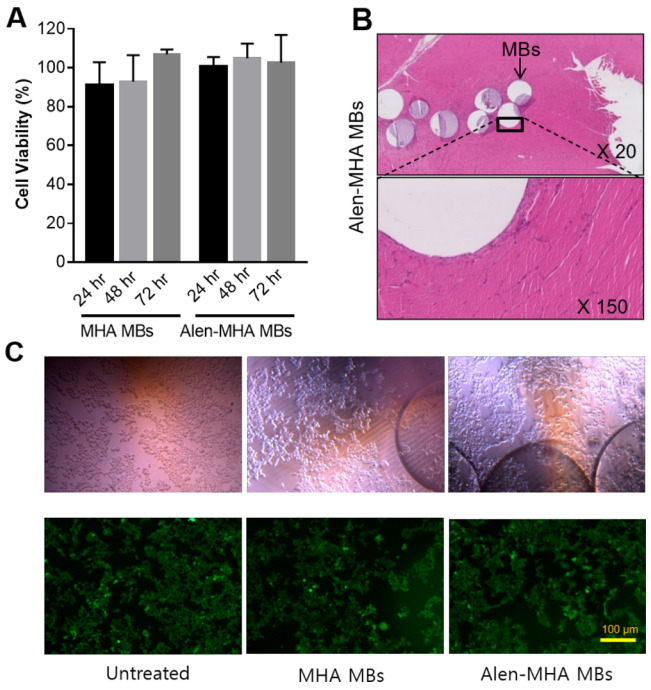

Figure 4. Cell and tissue compatibility of Alen-MHA MBs. (A) MC3T3-E1 cellular toxicity of MHA and Alen-MHA MBs ($n = 3$, mean ± sd). (B) Tissue compatibility of Alen-MHA MBs after implantation of the rat thigh muscle. Magnification ×20 and ×150 are shown. (C) Live and dead cell staining images after treatment with MHA and Alen-MHA MBs.

Moreover, the tissue compatibility of Alen-MHA MBs was observed after the *in vivo* implantation of Alen-MHA MBs on the rat leg muscle. As shown in Figure 4B, the histology micrographs, observed after 2 weeks of implantation, showed no obvious broken cells or irregular shape of cells at the interface between the Alen-MHA MBs and local tissues, indicating that there was no significant acute inflammatory response or severe fibrotic deformation of muscle tissues.

The tissue compatibility of HA alone or crosslinked HA has been confirmed in various preclinical and clinical assessments. Based on the tissue compatibility data, we confirmed that Alen-MHA BMs can be used as a safe drug carrier of BMP2 and can be applied to muscle and bone tissues for therapy.[30]

3.5. Cellular Osteogenic Activity of BMP2/Alen-MHA MBs by Treatment Design. In this study, we observed the gene expression levels of osteoblastic markers (*RUNX2*, *ALP*, and *OCN*) in MC3T3-E1 cells after BMP2/Alen-MHA MB treatment. As shown in Figure 5A, the expression of *Alp* and *Runx2* mRNA showed equivalent values between the single treatment (4 MBs, 1 time treatment for 12 days) and the multiple treatment (1 MB for every 3 days; four times treatment for 12 days). However, the gene expression of *Ocn* in single treatment was lower than that in multiple treatment (5.80 ± 0.84 vs 2.11 ± 0.05, $p \leq 0.01$). Alizarin Red S staining performed on day 12 showed higher mineralization in the multiple treatment than in the single treatment.

3.6. Bone Formation Efficacy of BMP2/Alen-MHA MBs. In this study, BMP2 alone, Alen-MHA MBs, and BMP2/Alen-MHA MBs were introduced to the thigh muscle pouches of mice, and bone formation in the thigh muscle pouches was observed using micro-CT (Figure 6). Figure 6A shows distinct bone formation in the groups of BMP2 and BMP2/Alen-MHA MBs compared with that in the control treatments (Alen-MHA MB group and untreated group). In the BMP2/Alen-MHA MB and BMP2 groups, the BMP2/Alen-MHA MB group showed a more palpable bone mass than that found with the BMP2 treatment. H&E and MT staining also showed that bone formation was more significant in the BMP2/Alen-MHA MBs than in the other groups (Figure 6B,C). Generally, BMP2 has a short half-life *in vivo*, averaging 7−16 min systemically.[31] Therefore, the MBs may act as a carrier, enabling the growth factor to be gradually released.

4. DISCUSSION

The application of BMP2 for the repair of large bone defects has become the most common treatment used after the first introduction of the product to the market in 2002.[32] Despite outstanding bone-induction efficacy, BMP2 and its delivery systems have been associated with numerous complications, including hyperplasia of the surrounding tissues, angiogenesis, soft tissue inflammation, and unexpected (ectopic and heterotopic) ossification.[7] These major components are known to be mainly from off-label applications or high-dose applications.[33,34] Commercial BMP2 delivery systems typically involve the adsorption of BMP2 to a vehicle scaffold (i.e., collagen sponge and tricalcium phosphate powder) to localize the protein to bone defects. However, these scaffolds do not have specific affinity for BMP2, cannot retain the protein within the system, and inevitably induce uncontrolled diffusion of BMP2 to the surrounding tissues, leading to serious complications. Consequently, efforts to ensure the therapeutic efficacy and safety of BMP2 are being developed by optimizing delivery carriers. In this study, as shown in Figures 1 and 2, we designed anionic polyelectrolyte MBs for ionic interaction-based BMP2 delivery. Methacrylated hyaluronate was chemically conjugated with Alen, which has two phosphonates [$PO(OH)_2$] in the molecule, and was further introduced into photo-crosslinking capillary microfluidics to obtain BMP2 carrying Alen-MHA MBs. Subsequent experiments (Figure 3A, absorption of FITC-BMP2 to Alen-MHA MBs) proved that the ionic−charge interaction of BMP2 was much stronger for Alen-MHA MBs than for MHA MBs. The estimated drug loading efficiency was over 85% after 5 h of incubation (Figure 3C).

https://doi.org/10.1021/acs.biomac.1c00610
Biomacromolecules 2021, 22, 4138−4145

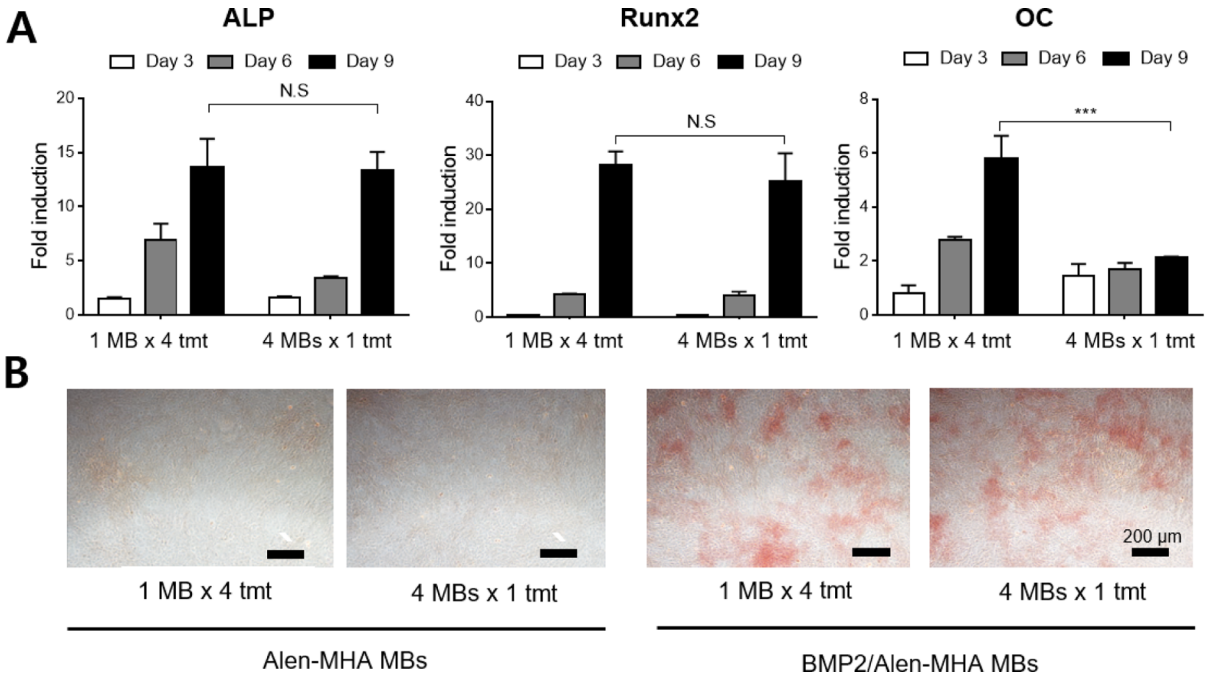

Figure 5. Cellular induction of osteogenic marker genes. (A) MC3T3-E1 cellular induction of osteogenic markers: runt-related transcription factor 2 (*Runx2*), alkaline phosphatase (*Alp*), and osteocalcin (*Ocn*) under different treatment protocols of BMP2/Alen-MHA MBs. Error bars indicate the standard error of the mean (S.E.M.) for $n = 3$ (p-values, acquired by the Student t-test, are summarized as such: ***, $p < 0.001$; ns, no significant difference). (B) Alizarin Red S staining of MC3T3-E1 cells after 12 days of incubation with Alen-MHA MBs and BMP2/Alen-MHA MBs. (Note: tmt = treatment).

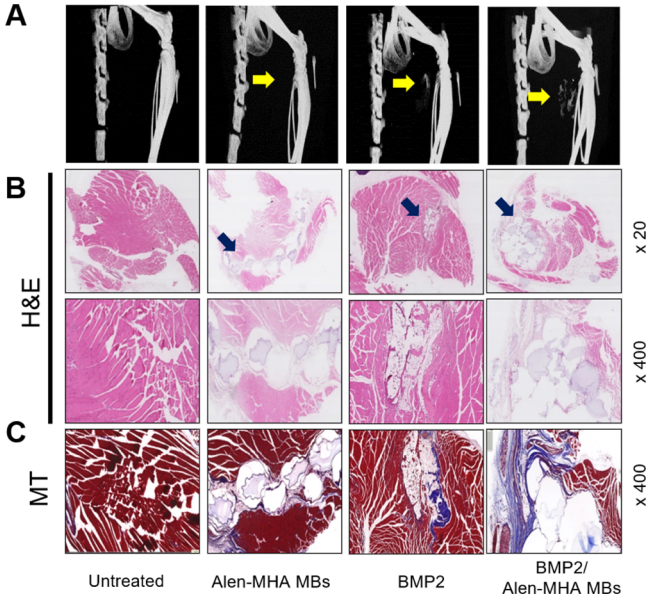

Figure 6. Bone formation efficacy under the treatment of BMP2/Alen-MHA MBs. (A) Microcomputed tomography of rat thigh muscles after the implantation of BMP2/Alen-MHA MBs. Yellow arrow indicates the implant site and bone formation. (B,C) Hematoxylin and eosin and Masson trichrome staining of muscle tissues after 4 weeks of treatment of BMP2/Alen-MHA MBs. Black arrows indicate the implantation site.

Jiskoot et al. reported the occurrence of eight cancer cases in patients after 2 years of follow-up of a 40 mg high-dose BMP2 trial. However, doses of BMP2 at 6 and 12 mg did not enhance the risk of cancer.[35] These reports suggest that the release control of BMP2 is a major factor for BMP2-related complications, especially in the case of high-dose treatment. Our data show that the release of BMP2 from Alen-MHA MBs can be controlled by ionic interaction mechanisms. The release profile, measured directly by ELISA, demonstrated that approximately 60% of BMP2 was released over the course of 10 days (Figure 3D). BMP2-related complications seem to be avoided if we can control the daily delivery dose of BMP2 in the optimal range. However, the safe range for daily dosage or optimized local tissue concentration of BMP2 has not been well defined.

To prove our hypothesis, we investigated the effect of controlled treatment on cellular mineralization by comparing the expression levels of osteogenic genes (*Alp*, *Runx2*, and *Ocn*) between the multiple treatment (1 MB × 4 treatment) and single treatment (4 MBs × 1 treatment). As shown in Figure 5, the induction levels of Alp and Runx2 mRNA in single treatment and multiple treatment did not show a statistical difference. However, Alizarin Red S staining and OC expression levels in multiple treatment were higher than those in the single treatment. In the process of osteogenic differentiation, the *Alp* gene was expressed slowly and increased to a maximum level when the cells underwent matrix maturation and then decreased at the mineralization stage. The *Runx-2* gene was expressed early in osteogenesis. OCN is a late bone marker that plays a key role in bone mineral disposition in the final stages of osteogenesis. The genes for these three markers may be expressed continually during osteogenesis.[36,37] Our data also suggest that the low dose (125 ng of BMP2) and multiple treatments, which can be represented by the "controlled delivery of BMP2", were more efficient in cellular osteoblastic gene induction (Figure 5). In this respect, polyelectrolyte Alen-MHA MBs, which display well-controlled BMP2 loading and release, can be a more reliable delivery design to ensure the efficacy and safety of BMP2.

In animal studies, controlled dose BMP2 treatment with Alen-MHA MBs was more potent and enhanced the *in vivo* bone

https://doi.org/10.1021/acs.biomac.1c00610
Biomacromolecules 2021, 22, 4138−4145

formation compared with that of BMP2 alone (Figures 6 and S6). This result indicated that the sustained delivery of BMP2 was more effective than only using BMP2 for bone formation. Furthermore, MT and H&E staining also showed that similar areas of bone fusion were present in rats treated with either BMP2 only or BMP2/Alen-MHA MBs.

5. CONCLUSIONS

In this study, we present a platform design for a BMP2 delivery system in the form of polyelectrolyte Alen-MHA MBs that display well-controlled loading and release of BMP2 via the ionic interaction mechanism. We propose that BMP2 loading and release can be tuned by extending the conjugation of bisphosphonate. Given that the uncontrolled release of BMP2 from current commercial products, such as collagen sponge, is a major limitation undermining the safety and efficacy of BMP2 treatments, Alen-MHA MBs may address the safety issues of scaffold-based BMP2 delivery systems. Hence, BMP2/Alen-MHA MBs could be a potent platform design for BMP2-related orthopedic procedures.

■ ASSOCIATED CONTENT

Supporting Information

The Supporting Information is available free of charge at https://pubs.acs.org/doi/10.1021/acs.biomac.1c00610.

Schematic representation of the reaction of MHA and Alen-MHA; ^{1}H NMR spectra of HA, TBA, HA TBA, MHA and Alen-MHA; FTIR spectra of HA, MHA, Alen-MHA (bead), and Alen-MHA (powder); ICP-OES assay of calibration, Alen, Alen-MHA MBs for quantification of the phosphorus content; size distribution of (A) MHA and (B) Alen-MHA; rat spinal fusion efficacy of BMP-2/Alen-MHA MBs; Masson trichrome staining of spinal cord after treatment of Alen-MHA MBs and BMP-2/Alen-MHA MBs; histology of spinal bones after fusion studies; and fusion scores obtained using physical palpation (Student's t-test, $n = 3$, $^*p < 0.1$) (PDF)

■ AUTHOR INFORMATION

Corresponding Author

Su-Geun Yang − *Department of Biomedical Science, BK21 FOUR Program in Biomedical Science and Engineering, Inha University College of Medicine, Incheon 22212, South Korea; Inha Institute of Aerospace Medicine, Inha University College of Medicine, Incheon 22332, South Korea;* orcid.org/0000-0001-5278-8723; Phone: +82-32-890-2832; Email: sugeun.yang@inha.ac.kr; Fax: +82-32-890-1199

Authors

Ratchapol Jenjob − *Department of Biomedical Science, BK21 FOUR Program in Biomedical Science and Engineering, Inha University College of Medicine, Incheon 22212, South Korea*

Hong-Phuong Nguyen − *Department of Biomedical Science, BK21 FOUR Program in Biomedical Science and Engineering, Inha University College of Medicine, Incheon 22212, South Korea; Institute of Research and Development, Duy Tan University, Da Nang 550000, Vietnam*

Min-Kyoung Kim − *Department of Biomedical Science, BK21 FOUR Program in Biomedical Science and Engineering, Inha University College of Medicine, Incheon 22212, South Korea*

Yixin Jiang − *Department of Biomedical Science, BK21 FOUR Program in Biomedical Science and Engineering, Inha University College of Medicine, Incheon 22212, South Korea; Inha Institute of Aerospace Medicine, Inha University College of Medicine, Incheon 22332, South Korea*

Jung Joo Kim − *Department of Biomedical Science, BK21 FOUR Program in Biomedical Science and Engineering, Inha University College of Medicine, Incheon 22212, South Korea*

Complete contact information is available at: https://pubs.acs.org/10.1021/acs.biomac.1c00610

Author Contributions

R.J., H-P.N., and M-K.K. contributed equally to this work. R.J., H-P.N., and M-K.K.: methodology and investigation. Y.J.: formal analysis and investigation. J.J.K.: writing—review and editing. S-G.Y.: conceptualization, validation, supervision, writing—review and editing, and project administration.

Notes

The authors declare no competing financial interest.

■ ACKNOWLEDGMENTS

This work was supported by the Basic Science Research Program, Brain Pool Program, and the Bio & Medical Technology Development Program of the National Research Foundation (NRF) funded by the Korean government (MOE and MSIT) (2020R1A2B5B02002377, 2018R1A6A1A03025523, 2021H1D3A2A02045561, and 2019M3E5D1A02069623).

■ REFERENCES

(1) Seeherman, H.; Wozney, J. M. Delivery of bone morphogenetic proteins for orthopedic tissue regeneration. *Cytokine Growth Factor Rev.* **2005**, *16*, 329−345.

(2) Urist, M. R. Bone: formation by autoinduction. *Science* **1965**, *150*, 893−899.

(3) Salazar, V. S.; Gamer, L. W.; Rosen, V. BMP signalling in skeletal development, disease and repair. *Nat. Rev. Endocrinol.* **2016**, *12*, 203−221.

(4) Anderson, C. L.; Whitaker, M. C. Heterotopic ossification associated with recombinant human bone morphogenetic protein-2 (infuse) in posterolateral lumbar spine fusion: a case report. *Spine* **2012**, *37*, E502−E506.

(5) Miyazawa, K.; Kawai, T.; Urist, M. R. Bone morphogenetic protein-induced heterotopic bone in osteopetrosis. *Clin. Orthop. Relat. Res.* **1996**, *324*, 259−267.

(6) Stoeger, T.; Proetzel, G. E.; Welzel, H.; Papadimitriou, A.; Dony, C.; Balling, R.; Hofmann, C. In situ gene expression analysis during BMP2-induced ectopic bone formation in mice shows simultaneous endochondral and intramembranous ossification. *Growth Factors* **2002**, *20*, 197−210.

(7) James, A. W.; LaChaud, G.; Shen, J.; Asatrian, G.; Nguyen, V.; Zhang, X.; Ting, K.; Soo, C. A Review of the Clinical Side Effects of Bone Morphogenetic Protein-2. *Tissue Eng., Part B* **2016**, *22*, 284−297.

(8) Zara, J. N.; Siu, R. K.; Zhang, X.; Shen, J.; Ngo, R.; Lee, M.; Li, W.; Chiang, M.; Chung, J.; Kwak, J.; Wu, B. M.; Ting, K.; Soo, C. High doses of bone morphogenetic protein 2 induce structurally abnormal bone and inflammation in vivo. *Tissue Eng., Part A* **2011**, *17*, 1389−1399.

(9) Huang, H.; Feng, J.; Wismeijer, D.; Wu, G.; Hunziker, E. B. Hyaluronic Acid Promotes the Osteogenesis of BMP-2 in an Absorbable Collagen Sponge. *Polymers* **2017**, *9*, 339.

(10) Mumcuoglu, D.; Fahmy-Garcia, S.; Fahmy-Garcia, S.; Ridwan, Y.; Nicke, J.; Farrell, E.; Kluijtmans, S.; van Osch, G. J. Injectable BMP-2 delivery system based on collagen-derived microspheres and alginate induced bone formation in a time- and dose-dependent manner. *Eur. Cells Mater.* **2018**, *35*, 242−254.

(11) Mirmohseni, F.; Cheng, T.; Oveissi, F.; Behi, M.; Schindeler, A.; Little, D.; Naficy, S.; Dehghani, F.; Valtchev, P. Optimized Synthesis of Poly(deoxyribose) Isobutyrate, a Viscous Biomaterial for Bone Morphogenetic Protein-2 Delivery. *ACS Appl. Mater. Interfaces* **2019**, *11*, 2870−2879.
(12) Maisani, M.; Sindhu, K. R.; Fenelon, M.; Siadous, R.; Rey, S.; Mantovani, D.; Chassande, O. Prolonged delivery of BMP-2 by a non-polymer hydrogel for bone defect regeneration. *Drug Delivery Transl. Res.* **2018**, *8*, 178−190.
(13) Krishnan, L.; Priddy, L. B.; Esancy, C.; Klosterhoff, B. S.; Stevens, H. Y.; Tran, L.; Guldberg, R. E. Delivery vehicle effects on bone regeneration and heterotopic ossification induced by high dose BMP-2. *Acta Biomater.* **2017**, *49*, 101−112.
(14) Cheng, G.; Yin, C.; Tu, H.; Jiang, S.; Wang, Q.; Zhou, X.; Xing, X.; Xie, C.; Shi, X.; Du, Y.; Deng, H.; Li, Z. Controlled Co-delivery of Growth Factors through Layer-by-Layer Assembly of Core-Shell Nanofibers for Improving Bone Regeneration. *ACS Nano* **2019**, *13*, 6372−6382.
(15) Nielsen, J. J.; Low, S. A. Bone-Targeting Systems to Systemically Deliver Therapeutics to Bone Fractures for Accelerated Healing. *Curr. Osteoporos. Rep.* **2020**, *18*, 449−459.
(16) Aderibigbe, B.; Aderibigbe, I.; Popoola, P. Design and Biological Evaluation of Delivery Systems Containing Bisphosphonates. *Pharmaceutics* **2016**, *9*, 2−25.
(17) Ochiuz, L.; Grigoras, C.; Popa, M.; Stoleriu, I.; Munteanu, C.; Timofte, D.; Profire, L.; Grigoras, A. G. Alendronate-Loaded Modified Drug Delivery Lipid Particles Intended for Improved Oral and Topical Administration. *Molecules* **2016**, *21*, 858−873.
(18) Sasaki, T.; Watanabe, C. Stimulation of osteoinduction in bone wound healing by high-molecular hyaluronic acid. *Bone* **1995**, *16*, 9−15.
(19) Han, D.; Liu, W.; Ao, Q.; Wang, G. Optimal delivery systems for bone morphogenetic proteins in orthopedic applications should model initial tissue repair structures by using a heparin-incorporated fibrin-fibronectin matrix. *Med. Hypotheses* **2008**, *71*, 374−378.
(20) Jing, D.; Hao, X.; Xu, F.; Liu, J.; Xu, F.; Luo, E.; Meng, G. Effects of local delivery of BMP2, zoledronate and their combination on bone microarchitecture, biomechanics and bone turnover in osteoporotic rabbits. *Sci. Rep.* **2016**, *6*, 28537.
(21) Pedrosa, S. S.; Goncalves, C.; David, L.; Gama, M. A novel crosslinked hyaluronic acid nanogel for drug delivery. *Macromol. Biosci.* **2014**, *14*, 1556−1568.
(22) Kim, M. K.; Kim, M. A.; Jenjob, R.; Lee, D. H.; Yang, S. G. Capillary microfluidics-derived doxorubicin-containing human serum albumin microbeads for transarterial chemoembolization of hepatic cancer. *Mater. Sci. Eng., C* **2016**, *62*, 391−397.
(23) Kim, M. K.; Lee, H. N.; Jenjob, R.; Lee, J.; Yang, S. G. Calcium-Triggered Pulsatile Delivery of Parathyroid Hormone from Microbeads for Osteoporosis Treatment. *Biomacromolecules* **2017**, *18*, 3099−3105.
(24) Gattas-Asfura, K. M.; Naistat, D. M.; Leblanc, R. M. Color change of toluidine blue induced by polyanionic quantum dots. *Colloids Surf., A* **2006**, *282*, 471−474.
(25) Tellier, L. E.; Miller, T.; McDevitt, T. C.; Temenoff, J. S. Hydrolysis and sulfation pattern effects on release of bioactive bone morphogenetic protein-2 from heparin-based microparticles. *J. Mater. Chem. B* **2015**, *3*, 8001−8009.
(26) Yoon, B. H.; Esquivies, L.; Ahn, C.; Gray, P. C.; Ye, S. K.; Kwiatkowski, W.; Choe, S. An activin A/BMP2 chimera, AB204, displays bone-healing properties superior to those of BMP2. *J. Bone Miner. Res.* **2014**, *29*, 1950−1959.
(27) Arzeno, A.; Wang, T.; Huddleston, J. I., 3rd Abundant heterotopic bone formation following use of rhBMP-2 in the treatment of acetabular bone defects during revision hip arthroplasty. *Arthroplast. Today* **2018**, *4*, 162−168.
(28) Dimar, J. R., II; Glassman, S. D.; Burkus, J. K.; Pryor, P. W.; Hardacker, J. W.; Carreon, L. Y. Reply to A critical review of recombinant human bone morphogenetic protein-2 trials in spinal surgery: emerging safety concerns and lessons learned. *Spine J.* **2011**, *11*, 1082−1083 ; author reply 1083-6.
(29) Sridharan, G.; Shankar, A. A. Toluidine blue: A review of its chemistry and clinical utility. *J. Oral Maxillofac. Pathol.* **2012**, *16*, 251−255.
(30) Wang, W.; Fan, M.; Zhang, L.; Liu, S. H.; Sun, L.; Wang, C. Y. Compatibility of hyaluronic acid hydrogel and skeletal muscle myoblasts. *Biomed. Mater.* **2009**, *4*, 025011.
(31) Khattar, V.; Lee, J. H.; Wang, H.; Bastola, S.; Ponnazhagan, S. Structural determinants and genetic modifications enhance BMP2 stability and extracellular secretion. *FASEB BioAdv.* **2019**, *1*, 180−190.
(32) McKay, W. F.; Peckham, S. M.; Badura, J. M. A comprehensive clinical review of recombinant human bone morphogenetic protein-2 (INFUSE Bone Graft). *Int. Orthop.* **2007**, *31*, 729−734.
(33) Ong, K. L.; Villarraga, M. L.; Lau, E.; Carreon, L. Y.; Kurtz, S. M.; Glassman, S. D. Off-label use of bone morphogenetic proteins in the United States using administrative data. *Spine* **2010**, *35*, 1794−1800.
(34) Smucker, J. D.; Rhee, J. M.; Singh, K.; Yoon, S. T.; Heller, J. G. Increased swelling complications associated with off-label usage of rhBMP-2 in the anterior cervical spine. *Spine* **2006**, *31*, 2813−2819.
(35) El Bialy, I.; Jiskoot, W.; Reza Nejadnik, M. Formulation, Delivery and Stability of Bone Morphogenetic Proteins for Effective Bone Regeneration. *Pharmaceut. Res.* **2017**, *34*, 1152−1170.
(36) Ducy, P.; Zhang, R.; Geoffroy, V.; Ridall, A. L.; Karsenty, G. Osf2/Cbfa1: a transcriptional activator of osteoblast differentiation. *Cell* **1997**, *89*, 747−754.
(37) Mao, Z.; Li, Y.; Yang, Y.; Fang, Z.; Chen, X.; Wang, Y.; Kang, J.; Qu, X.; Yuan, W.; Dai, K.; Yue, B. Osteoinductivity and Antibacterial Properties of Strontium Ranelate-Loaded Poly(Lactic-co-Glycolic Acid) Microspheres With Assembled Silver and Hydroxyapatite Nanoparticles. *Front. Pharmacol.* **2018**, *9*, 368.

https://doi.org/10.1021/acs.biomac.1c00610
Biomacromolecules 2021, 22, 4138−4145